

# Influence of Disc Degeneration on Mechanism of Thoracolumbar Burst Fractures

OSAMU SHIRADO, MD,\* KIYOSHI KANEDA, MD,\* SHIGERU TADANO, PhD,†  
HIROMASA ISHIKAWA, PhD,† PAUL C. McAFEE, MD,‡  
and KAREN E. WARDEN, M Biomed Eng‡

**In order to clarify the pathomechanism of thoracolumbar burst fractures and to evaluate the influence of disc degeneration and bone mineral density, a biomechanical study was performed using cadaveric spines. Eleven motion segments of thoracolumbar spines from human cadavers were compressed vertically until a fracture occurred. In addition, bone mineral density and degree of disc degeneration were determined for each specimen. Compression of 7 of 11 specimens resulted in the typical burst fracture characterized by retropulsion of a bony fragment into the spinal canal and an increase of the interpedicular distance. All seven specimens showed disruptions of the middle end plate and disc materials in the vertebral body. The fracture line was located between the middle of the end plate and the middle of the posterior wall cortex. No burst fractures were seen in the specimens with severely degenerated discs and osteoporosis. In order to confirm the stress state in a vertebra that induces the burst fracture, finite element analysis of one motion segment was also carried out under the same mechanical conditions as the experiments in this study. As a result of calculation for the healthy disc, the highest stresses under axial compression were concentrated in the following areas: the middle of the end plate, the cancellous bone under the nucleus pulposus, and the middle of the posterior wall cortex. This implies that the above regions are more vulnerable to vertical compressive load. In the analysis of specimens with severely degenerated discs, stresses were very low at the end plate and cancellous bone under the nucleus. Therefore, axial compression was reconfirmed as inducing typical burst fractures in the thoracolumbar spine. Moreover, the mechanism of this fracture was influenced by disc degeneration and bone mineral density. [Key words: mechanism, burst fracture, disc degeneration, osteoporosis, thoracolumbar spine]**

**B**URST FRACTURE, in which the most characteristic findings are the comminution of the vertebral body and retropulsed bony fragment into the spinal canal, is one of the most common injuries in the thoracolumbar spine.<sup>2,12,17</sup> This type of fracture is not likely to occur and produce neurologic deficits in the very elderly, who usually have a degenerated disc and osteoporosis.<sup>20,22</sup>

Holdsworth<sup>11</sup> first reported the concept of thoracolumbar burst

fracture in 1963. He divided the spinal column into anterior and posterior columns, and stated that the burst fracture is caused by compression and therefore is a stable injury, although he did not make any reference to the bone fragment in the canal. With the development of computed tomography (CT), Denis<sup>2</sup> and McAfee et al<sup>17</sup> proposed a new classification of the thoracolumbar spinal injury based on the three-column theory. The anterior column is formed by the anterior longitudinal ligament, anterior annulus fibrosus, and anterior part of the vertebral body. The middle one consists of the posterior longitudinal ligament, posterior annulus fibrosus, and posterior wall of vertebral body. The posterior one involves the posterior bony complex alternating with the posterior ligamentous complex. Using this classification, Denis<sup>2</sup> and McAfee et al<sup>17</sup> pointed out the pathogenesis of the burst fracture as failure of the anterior and middle columns under axial compression. They also emphasized that the retropulsed bone fragment could be a key factor in terms of diagnosis and treatment. The treatment, whether conservatively or surgically, has been recently discussed in orthopaedic literature.<sup>2,3,6,11,16,17</sup> There are, however, few articles concerning the mechanism of the burst fracture, especially on a predictive basis.<sup>21</sup> It is also important to know the pathomechanism of the fracture from a clinical standpoint.

The goals of this study were twofold:

1. To clarify the pathomechanism of thoracolumbar burst fractures with special reference to the occurrence of retropulsed bony fragments into the spinal canal.
2. To evaluate the influence of disc degeneration and osteoporosis on the mechanism of the burst fracture.

## MATERIALS AND METHODS

**Vertical Compression Test with Human Cadaveric Spines.** Eleven spinal segments consisting of two vertebrae and one intervening disc were harvested from autopsy, and immediately frozen at  $-20^{\circ}\text{C}$  in double-thickness plastic bags. All spinal segments were obtained from individuals who had died of acute diseases such as myocardial infarction and cerebrovascular injury. The age of specimens ranged from 30 to 75 years, with an average age of 52 years. The levels of specimens were as follows: two from T10–11, three from T12–11, three from L2–3, and three from L4–5. Just before the compression test, all specimens were thawed to room temperature. The surrounding soft tissue and muscle were dissected off each specimen, with great care being taken to preserve the osseous and ligamentous structure. All specimens were kept moist during dissection and testing, and the total time of preparing and testing the specimens never exceeded 1 hour.

Dual photon absorptiometry (DPA) studies were performed *in vitro* by placing each of the 11 vertebral segments in a saline bath just before biomechanical testing.<sup>5,9</sup> The scans were performed using commercially available techniques—dichromatic photon absorptiometry for *in vitro* measurement of bone mineral density of the spine using a gadolinium-153 source emitting photons of 44 and 100 keV energy. The procedures were performed with the Lunar 3 software programs (Lunar Radiation Corporation, Madison, Wisconsin). The bone mineral den-

From the \*Department of Orthopaedic Surgery, Hokkaido University School of Medicine, and the †Department of Mechanical Engineering II, Hokkaido University, Sapporo, Japan, and the ‡Department of Orthopaedic Surgery, The Johns Hopkins University School of Medicine, Baltimore, Maryland.

Supported in part by NIH grant AR38489 and an OREF Career Development Award.

Accepted for publication January 7, 1991.

The authors thank Dewei Zou, MD for his help in performing the biomechanical study with cadavers.

sity (BMD;  $g/cm^2$ ) was calculated from the bone mineral content divided by the projected vertebral body area. Before determining BMD, anteroposterior and lateral radiographs of each vertebral segment were taken to exclude specimens with occult changes such as fractures, metastases, and the other bony abnormalities.

After determining BMD and taking radiographs, all motion segments were compressed axially until a fracture occurred by using a biaxial servocontrolled MTS 858 Bionix hydraulic materials testing machine (Minneapolis, Minnesota). The cartridges of maximum load and displacement were 10,000 N axial compressive load and 20 mm axial linear displacement, respectively. The vertical compressive load was conducted by a ramp wave of 50 seconds up to 8,000 N. Between and among specimens, the rate of loading was kept constant at 160 N/second. The specimens were placed between parallel metal plates, which were mounted on a materials testing machine. Axial load and displacement were recorded through an analog-to-digital converter (DASH 16; Metrabyte, Taunton, Massachusetts) using an IBM XT computer. Six-channel bipolar recording was accomplished at 10 Hz, of 60 seconds' duration (ie, approximately 600 data points per channel). The computer files of biomechanical data could be directly imported through various commercially available software program<sup>5,7</sup> (Labtech Notebook, Wilmington, Massachusetts; Lotus Symphony, Cambridge, Massachusetts). The fractures could be found out on the load-deflection curve, that is, the load at fracture was determined at the peak of the curve. The specimens were unloaded immediately after the fracture, and anteroposterior and lateral radiographs were taken.

The motion segments were then cut into halves at the sagittal plane with a blade band saw. The cross-section was examined carefully, in terms of fracture line and disc condition. Finally, the intervening discs were graded into three groups according to the degree of macroscopic disc degeneration: normal disc, slightly and severely degenerated disc. Normal disc has a gelatinous nucleus pulposus easily distinguished from the annulus fibrosus. In the slightly degenerated disc, the nucleus was fibrotic but still soft. It was clearly distinguished from the annulus. In the severely degenerated disc, pronounced macroscopic changes occurred. Cavities were often seen in the nucleus. There was no visible boundary between the nucleus and the annulus.

**Computational Analysis for Lumbar Motion Segment.** Fractures usually occur when the stress becomes higher than the breaking strength

of a material. It is, therefore, very important to confirm the stress state under a certain external load in order to estimate the mechanism of fractures.

A two-dimensional finite element model for plane strain analysis consists of two vertebral bodies and the intervening disc (one motion segment) (Figure 1A). We did not consider the posterior elements of vertebrae—pedicles, laminae, articular processes, spinous processes, and the other posterior ligaments. The geometry of a model was traced precisely on the lateral radiograph of an L3-4 specimen of a 42-year-old man, who died suddenly of brain injury. Figure 1B shows this finite element model (Model I), which contains two vertebral bodies and one intervertebral disc. This model has 754 triangular elements and 413 nodes, divided into five different mechanical substructures: cortical bone, cancellous bone, annulus fibrosus, nucleus pulposus, and anterior and posterior longitudinal ligaments. For the analysis, the mechanical effect of the cartilaginous end plate was assumed to be negligible.<sup>15,24</sup> Material properties of the substructures, shown in Table 1, are determined on the basis of previous reports.<sup>4,14,15,24,27</sup> Annulus fibrosus has been modeled as an isotropic elastic material and nucleus pulposus as a noncompressive and nonviscid fluid. Therefore, Poisson's ratio ( $\nu$ ) of the nucleus pulposus was considered to be 0.499999. Young's modulus (E) of the nucleus was calculated from the bulk modulus ( $K = 2,255$  MPa) and Poisson's ratio with the following formula<sup>23</sup>:

$$K = E/3(1 - 2\nu). \quad (1)$$

On the other hand, the severely degenerated disc was simulated with a model with an empty nucleus (Model II), because the nucleus becomes dehydrated with degeneration, and cavity formation is finally often seen clinically. The mechanism of thoracolumbar burst fractures might be influenced by BMD, as well as by disc degeneration. However, the same material properties as in Model I were used for the analysis of Model II, in order to evaluate the influence of the condition of the nucleus.

A compressive load of 30 N in unit thickness was applied to each node of the upper end plate in each model (Models I and II). Nachemson<sup>19</sup> discovered in his experiments that the internal pressure of the nucleus in the normal L3-4 disc is 1.5 times as much as the external pressure while compressed vertically. Therefore, 26 N was applied as a normal force to the outer nodes of the nucleus in Model I. The upper boundary of each model was fixed in the lateral direction, while the

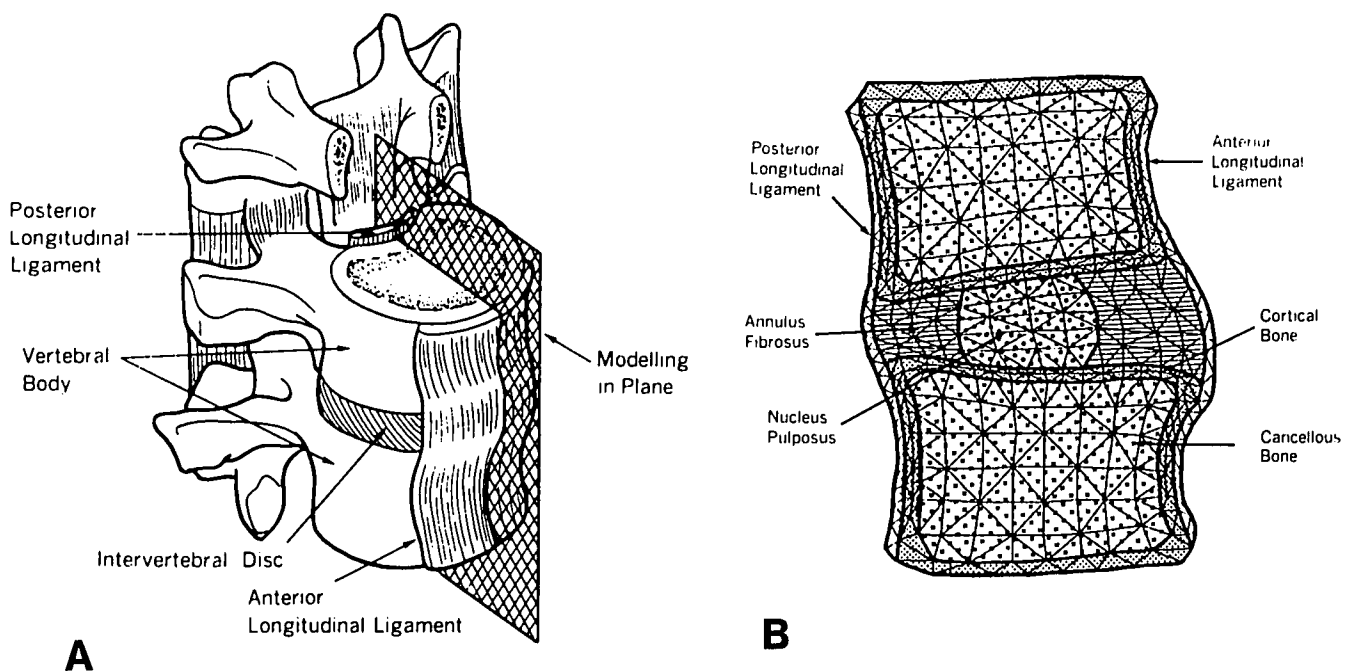


**Fig 1.** **A**, One motion segment of the lumbar spine to be considered for the computational analysis. The slice is located at the midsagittal portions through two vertebral bodies and an intervertebral disc. **B**, The plane model of the finite element method. There are 754 triangular plane elements and 413 nodes in this model. The heavy line shows the boundaries among the different substructures.

Table 1. Material Properties

Material	Young modulus (MPa)	Poisson Ratio
Cortical bone	12000	0.3
Cancellous bone	1500	0.2
Anulus fibrosus	10	0.4
Nucleus pulposus	0.013	0.499999
Ligament	40	0.4

lower one was free. Stress states in each element were expressed as effective stress, derived from the theory of Huber-Von Mises,<sup>23</sup> and can be used as a failure criterion.<sup>15</sup>

Results are shown in graphic form. The darker element in the mesh system represents the higher effective stress.

## RESULTS

### Macroscopic and Roentgenologic Observations of Fractured Vertebrae Caused by Axial Compression

A total of 11 motion segments was compressed vertically until a fracture occurred. The load-deflection curves were similar in most cases (Figure 2). During compression, the first crack was audible after the squeeze of blood and bone marrow from the nutritional foramina of the vertebral bodies. At the same time, the curve dropped slightly and began to rise immediately again. Little change in vertebral height could be seen at that time. The curve then reached a peak with a heavy cracking sound. Vertebral height was then reduced greatly.

Table 2 shows disc degeneration, BMD, and load at fracture for each specimen. Two of 11 specimens have a normal disc. Three specimens have a slightly degenerated disc, and six have a severely degenerated disc. The mean BMD was 0.820 g/cm<sup>2</sup>, which corresponded to 4,155 N of mean load at fracture. The lowest BMD was 0.618 g/cm<sup>2</sup> in specimen no. 2, which had a severely degenerated disc and fractured at 2,791 N; the highest was 1.034 g/cm<sup>2</sup> in specimen no. 10, which had a slightly degenerated disc and fractured at 5,356 N. The higher the BMD, the higher the tolerance of the specimen for compressive load. Although there was a small number of specimens, those with a higher BMD

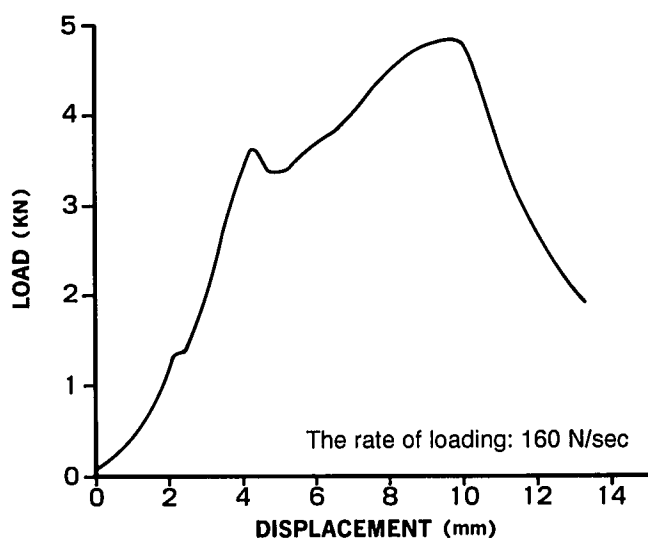


Fig 2. The load-deflection curve of specimen no. 7 (L2-3 segment) under axial compression. The rate of loading was 160 N/second. There are two peaks on the curve. The fracture occurred at the second peak.

fractured at a higher load, even among the same levels of motion segments.

Table 3 shows the results of macroscopic and roentgenologic observations of fractured vertebrae caused by axial compression. Seven of 11 specimens experienced the typical burst fracture, defined by Denis<sup>2</sup> and McAfee et al<sup>17</sup>: there was retropulsion of a bony fragment into the spinal canal from the crushed vertebral body and an increase of the interpedicular distance (Figure 3A,B). All burst fractures showed end-plate disruptions at the superior center or centeroposterior portion, and disc protrusion into the vertebral body. The fracture line fell between the superior end plate and the middle of the posterior wall cortex, in which the foramen of the basivertebral vein was located. In all seven specimens, the posterior longitudinal ligament was stripped from the posterior wall of the fractured vertebra due to a retropulsed bone fragment (Figure 3C). No transverse tear, however, was seen. Four of seven had posterior column injury such as facet or lamina fracture.

Regarding disc degeneration, burst fractures occurred in all five specimens with normal or slightly degenerated disc, versus only two of six with severely degenerated disc. Four of six were totally collapsed, and all four specimens had no end-plate disruptions (Figure 4A-C). There was no retropulsed bony fragment in the specimens with nonburst fractures.

In addition, all four specimens, except one, without burst fractures had lower BMDs (specimen no. 2: 0.618 g/cm<sup>2</sup>; no. 5: 0.667 g/cm<sup>2</sup>; no. 8: 0.727 g/cm<sup>2</sup>) compared with the other specimens. The more severely the disc degenerated, the lower the BMD tended to be.

### Stress Distribution of Lumbar Motion Segment Under Axial Compression

Stress analysis of vertebral bodies only is shown in Figures 5 and 6, as the destruction usually does not occur at the intervening disc, but at the vertebra (especially the lower one) of a motion segment under axial compression.<sup>2,3,12,16,17,21</sup> Figure 5A shows the stress distribution of the cancellous bone with the healthy disc (Model I). In the lower vertebra, the highest effective stresses were concentrated at the area under the nucleus pulposus and superoposterior to the vertebral body. Stress distribution of the cortical bone in the same model is shown in Figure 5B. The highest effective stresses can be seen at the region just under the nucleus and at the middle of the posterior wall of the vertebral body.

Small stresses were found under the nucleus pulposus in the model with a severely degenerated disc (Model II), although stresses in the posterior wall of the vertebral body increased (Figure 6A,B).

## DISCUSSION

The mechanism of thoracolumbar burst fractures was first investigated intensively in 1960 by Roaf.<sup>21</sup> One motion segment, including two vertebrae and one intervertebral disc, was compressed vertically in his study. He found that the end plate bulged more with increasing load and finally cracked in specimens from young adults. After this sequence, the nucleus pulposus was displaced into the vertebral body, which resulted in its disintegration with continued pressure. However, his study did not mention how the bony fragment was retropulsed into the spinal canal, or what was the relationship between the fragment and the end-plate fracture.

Thoracolumbar burst fractures occur less commonly in the very elderly with osteoporosis and a degenerated disc, because the vertebral fracture seen in conjunction with osteoporosis called compression fracture, usually involves only the anterior column, and is not generally associated with serious neurologic sequelae.<sup>20,22</sup> Kaneda et al<sup>13</sup> recently reported 10 osteoporotic patients who had vertebral body fractures resulting in neurologic complications. In five patients, however, it could not be decided if the initial fracture type was burst or compression

Table 2. Disc Degeneration, Bone Mineral Density, and Load at Fracture

Specimen No.	Level of Motion Segment	Disc Degeneration	Bone Mineral Density* (g/cm <sup>2</sup> )	Load at Fracture (N)
1	T10-11	Severe	0.899	5290
2	T10-11	Severe	0.618	2791
3	T12-L1	Severe	0.759	4719
4	T12-L1	Normal	0.869	3390
5	T12-L1	Severe	0.667	1938
6	L2-3	Normal	0.843	6390
7	L2-3	Slight	1.023	4887
8	L2-3	Severe	0.727	2367
9	L4-5	Slight	0.860	6090
10	L4-5	Slight	1.034	5356
11	L4-5	Severe	0.720	2490

\*Value of the lower vertebra before compression.  
N = Newtons.

because of advanced post-traumatic collapse. They concluded that post-traumatic collapse of the fractured vertebral body caused retropulsion of the vertebral fragment into the spinal canal. Hammerberg et al<sup>8</sup> also presented eight patients who had so-called senile burst fracture. All patients had trivial trauma or no initiating event.

We chose one motion segment of the thoracolumbar spine for the experimental study with cadaveric spines. White and Panjabi<sup>25</sup> proposed that the functional unit of the spine consisted of two vertebrae and one intervening disc, and that this unit was very useful for studying the biomechanics of the spine. So far, many authors have tested spines biomechanically using one motion segment.<sup>1,14,15,18,19,21,24,27</sup> Therefore, we believe that one motion segment provides an appropriate model for investigating the mechanism of spinal injuries. Since the *in vivo* boundary condition of the spines is unclear when the burst fracture occurs clinically, we simply put the specimens between the parallel metal plates and applied the pure compressive load with a materials testing machine.

The loading used in this study was static, whereas Willen et al<sup>26</sup> applied a dynamic load to obtain the burst fracture. The mechanism of a fracture might be different under static and dynamic loads. The experimental results in this study, however, simulated thoracolumbar burst fractures well. Seven of 11 specimens exhibited the typical burst

fracture under vertical compression. In those specimens, the end plate under the nucleus was broken, and the fracture line was located between the superior end plate and the middle of the posterior wall cortex, at the site of the foramen of the basivertebral vein. This foramen might weaken the vertebral body under compressive load. Disc material was displaced in the vertebral body.

Compared with two groups of specimens having a normal or a slightly degenerated disc, fewer specimens with a severely degenerated disc demonstrated burst fractures. In other words, the specimen with a severely degenerated disc was not likely to demonstrate burst fracture under compression. Although the number of specimens is too small for statistical analysis, our results correspond to the clinical findings; thoracolumbar burst fractures are rarely observed in very elderly people who have a severely degenerated disc. Roaf<sup>21</sup> found in his study that compression of specimens from older subjects did not induce the displacement of disc materials into the vertebral body, but entire vertebrae were collapsed. Willen<sup>26</sup> also pointed out this phenomenon.

With regard to bone density, no burst fractures occurred in the specimens with lower BMDs. Since there is some relationship between BMD and disc degeneration,<sup>9,10</sup> osteoporosis also might be one of the nonpredisposing factors in the mechanism of thoracolumbar burst fractures. Hansson et al<sup>10</sup> performed a biomechanical study in which

Table 3. Findings of Fractured (Fx) Lower Vertebra in Each Motion Segment

Specimen No.	End-Plate Fx and its Site	Disc protrusion into the Vertebral Body	Middle-Column* Lesion	Posterior-column† Lesion	Comment
1	—, Intact	—	—	—	No fx of the posterior wall cortex
2	—, Intact	—	+	—	Fx of the posterior wall cortex. No retropulsed bone fragment
3	+, Center	+	+	Facet fx	Burst fx (Denis type B‡)
4	+, Centroposterior	+	+	Lamina fx	Burst fx (Denis Type B)
5	—, Intact	—	+	—	Fx of the posterior wall cortex. No retropulsed bone fragment
6	+, Center	+	+	—	Burst fx (Denis Type B)
7	+, Centroposterior	+	+	Facet fx	Burst fx (Denis Type B)
8	—, Intact	—	+	—	Fx of the posterior wall cortex. No retropulsed bone fragment.
9	+, Center	+	+	—	Burst fx (Denis Type B)
10	+, Centroposterior	+	+	Facet fx	Burst fx (Denis Type A§)
11	+, Centroposterior	+	+	—	Burst fx (Denis Type A)

\*The posterior longitudinal ligament, anulus fibrosus, and posterior wall cortex.

†The posterior bony complex with the posterior ligaments.

‡Fracture of the superior endplate.

§Fracture of both endplates.



**Fig 3.** Lateral radiographs of specimen no. 7. **A**, Before compression. **B**, After compression. **C**, The sagittal cross-section of the specimen after being compressed vertically. **A,B**, The bony fragment (black arrow) retropulsed into the spinal canal can be seen at the superoposterior corner of the lower vertebra. A decrease in the vertebral height and facet fracture (white arrow) are also shown. **C**, The end plate is broken at the middle of the lower vertebra, and little disc material is displaced into the vertebral body. The fracture line is located between the middle of the end plate and the middle of the posterior wall cortex, where the foramen of the basivertebral vein is. The posterior longitudinal ligament is left intact.

one vertebra with 3-mm thick half discs covering the end plates were compressed vertically until fracture. Before mechanical testing, BMD and disc degeneration were estimated in each specimen. They classified three types of fractures, which depended on the BMD and disc degeneration. The end plate and cancellous bone under the nucleus were fractured in the specimens with healthy discs, which also demonstrated the higher BMD. On the other hand, the specimens with the severely degenerated disc had different types of fractures. Their findings also support the results of our study, although they did not use the same one-motion-segment model as ours, and did not consider the retropulsed bony fragment into the spinal canal.

Two-dimensional stress analysis in plane strain state was performed to estimate the stress distribution in the vertebral body under vertical compression. We analyzed the plane model of one motion segment, not including the posterior elements. The reasons for that are as follows: first, the geometry of vertebrae is symmetrical to the sagittal cross

section. Second, burst fractures under pure compression in this experiment occurred symmetrically to the sagittal plane. Finally, anterior components consisting of vertebral body and intervertebral disc play a significant role in resisting the vertical compressive load, which is regarded as the main force causing the burst fracture of thoracolumbar spines.<sup>27</sup>

This analysis was carried out with a static calculation that did not consider the rate-dependent property of each tissue, because our experimental results under static loading were comparable to the burst fractures that were seen clinically. Human thoracolumbar spines have complex contours and structure. Previous calculations using a finite element method, however, have been carried out with a very simplified model.<sup>14,15,24</sup> Our model was traced precisely from radiographs of the human lumbar spine.

The results of stress analysis corresponded well with the experimental results. In the model with a healthy disc, higher stresses could be

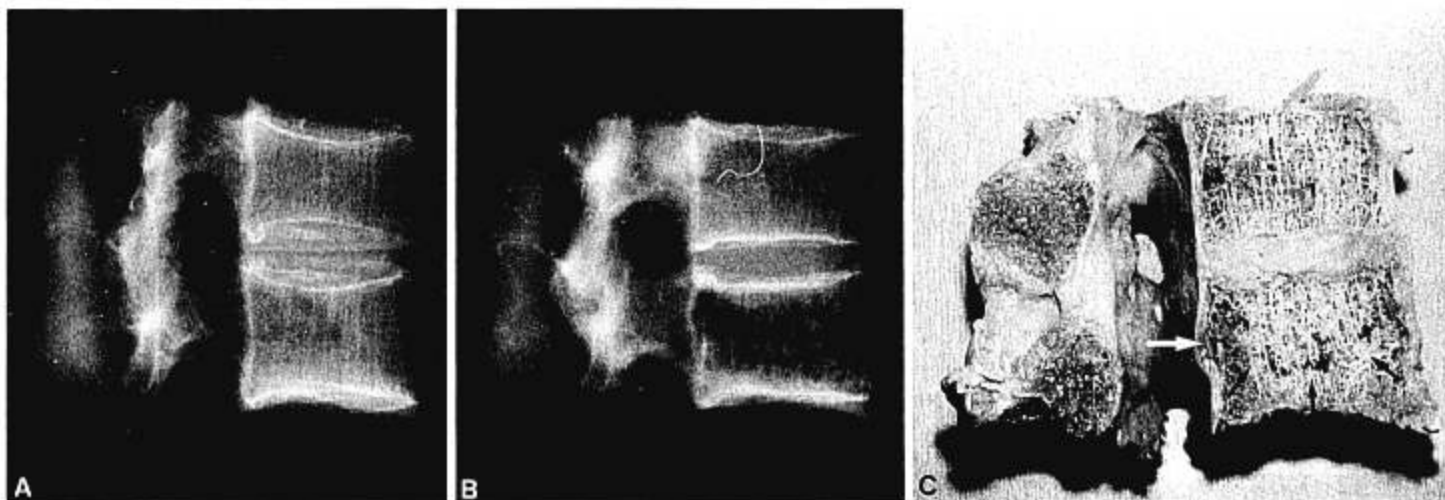


**Fig 4.** Lateral radiographs of specimen no. 5. **A**, Before compression. **B**, After compression. **C**, Sagittal cross-section of the specimen. Osteoporotic trabeculae are seen. The posterior wall cortex is broken (large arrow), although the end plate is left intact. **B**, There is no retropulsed bony fragment in the spinal canal. No end plate is broken. The cancellous bone is totally collapsed at the middle of the vertebral body (small arrows).

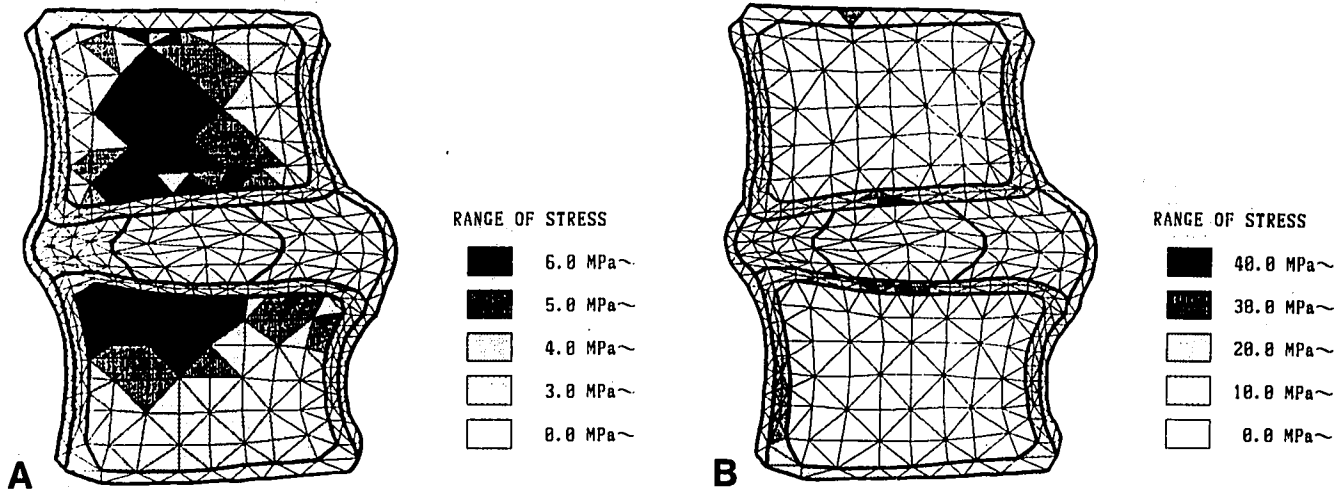


**Fig 5.** Stress distribution of one motion segment with a healthy disc (Model I) under axial compression. **A**, Effective stresses are shown in the spongy core. The highest ones are seen at the region under the nucleus and at the superoposterior portions. **B**, In the cortical shell, stresses are concentrated at the middle of the end plate and posterior wall cortex.

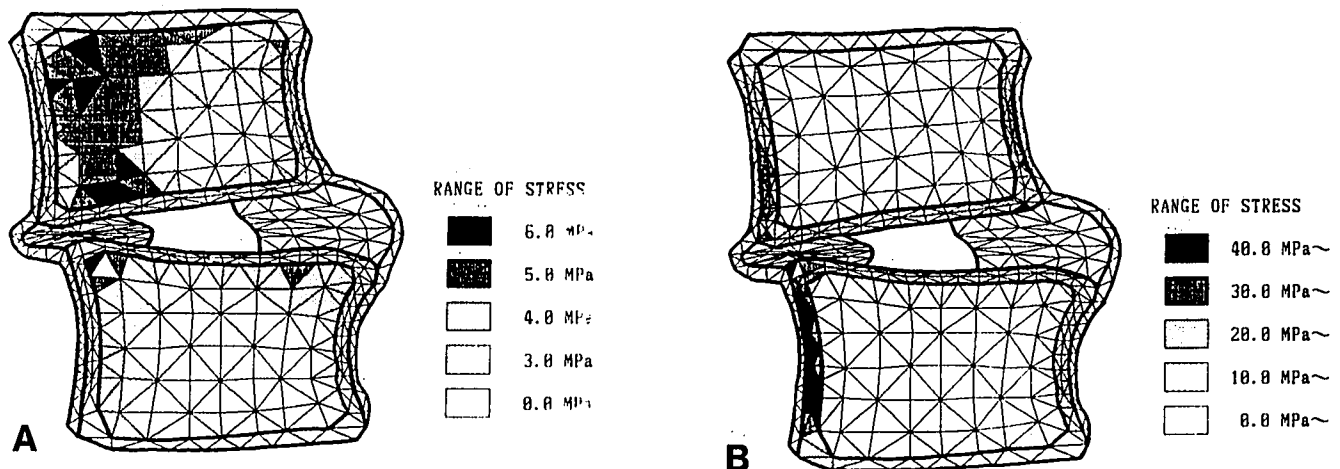


**Fig 6.** Stresses are shown in the model with a severely degenerated disc. **A**, In the spongy core, no stresses can be seen under the nucleus. **B**, There are a few stresses at the middle of the end plate, and the highest ones are at the posterior wall cortex.

seen in the following areas: the end plate and cancellous bone of the vertebral body under the nucleus pulposus, and the middle of the posterior wall cortex. This implies that the above regions are more vulnerable to axial compressive load. In the model with an empty nucleus to simulate the severely degenerated disc, little stress could be seen at the center of the end plate. This area is not likely to fail under compression.

In conclusion, it can be reconfirmed that axial compressive load induces typical burst fractures in the thoracolumbar spine. The end plate and cancellous bone located under the nucleus pulposus were broken, and the disc material was displaced into the vertebral body. The fracture line was located between the end plate and the middle of the posterior wall cortex. As a result, the bone fragment was retropulsed into the spinal canal. Thoracolumbar burst fracture with neurologic deficits is not likely to occur in the very elderly who have osteoporosis and a degenerated disc, because pathologic fractures due to senile osteoporosis usually involve only the anterior column.<sup>20,22</sup> In our experiments, few burst fractures occurred in the subjects with a severely degenerated

disc and osteoporosis. This implies that burst fractures occur less frequently in very elderly people.

## REFERENCES

1. Brinckmann P, Frobin W, Hierholzer E, Horst M: Deformation of the vertebral end-plate under axial loading of the spine. *Spine* 8:851-856, 1983
2. Denis F: The three column spine and its significance in the classification of acute thoracolumbar spinal injuries. *Spine* 8:817-831, 1983
3. Dickson JH, Harrington PR, Erwin WE: Results of reduction and stabilization of the severely fractured thoracic and lumbar spine. *J Bone Joint Surg* 60A:799-805, 1978
4. Evance FG, King AI: Mechanical properties of human bone Chap 3. *Biomechanical Studies of the Musculoskeletal System*. Edited by FG Evans. Springfield, IL, Charles C Thomas, 1961
5. Farey ID, McAfee PC, Gurr KR, Randolph MA: Quantitative histologic study of the influence of spinal instrumentation on lumbar fusions: A canine model. *J Orthop Res* 7:709-722, 1989
6. Flesh HR, Leider LL, Erickson DL, Chou SN, Bradford DS: Harrington instrumentation and spine fusion for unstable fracture and fracture-dislocation.

- tions of the thoracic and lumbar spine. *J Bone Joint Surg* 59A:143-153, 1977
7. Gurr KR, McAfee PC, Shih CM: Biomechanical analysis of anterior and posterior instrumentation systems after corpectomy: A calf-spine model. *J Bone Joint Surg* 70A:1182-1191, 1988.
  8. Hammerberg KW, DeWald RL: Senile burst fracture: A complication of osteoporosis. Presented at the annual meeting of the Scoliosis Research Society, Baltimore, Maryland, September 29-October 2, 1988
  9. Hansson T, Roos B, Nachemson A: The bone mineral content and ultimate compressive strength of lumbar vertebrae. *Spine* 5:46-55, 1980
  10. Hansson T, Roos B: The relation between bone mineral content, experimental compression fractures, and disc degeneration in lumbar vertebrae. *Spine* 6:147-153, 1981
  11. Holdsworth FW: Fractures, dislocations, and fracture-dislocations of the spine. *J Bone Joint Surg* 45B:6-20, 1963
  12. Kaneda K, Abumi K, Fujiya M: Burst fractures with neurologic deficits of the thoracolumbar-lumbar spine. *Spine* 9:788-795, 1984
  13. Kaneda K, Takahashi H, Abumi K, Hashimoto T, Nohara Y: Posttraumatic collapse of the vertebral body with neurologic complications in osteoporotic patients. Presented at the annual meeting of the Scoliosis Research Society, Baltimore, Maryland, September 29-October 2, 1988
  14. Kulak RF, Schultz AB, Belytschko T, Galante J: Biomechanical characteristics of vertebral motion segments and intervertebral discs. *Orthop Clin North Am* 1:121-133, 1975
  15. Kulowski P, Kubo A: The relationship of degeneration of the intervertebral disc to mechanical loading conditions on lumbar vertebrae. *Spine* 11:726-731, 1986
  16. McAfee PC, Yuan HA, Lasda NA: The unstable burst fracture. *Spine* 7:365-373, 1982
  17. McAfee PC, Yuan HA, Frederickson BE, Lubricky JP: The value of computed tomography in thoracolumbar fractures. *J Bone Joint Surg* 65A:461-473, 1983
  18. Nachemson A: Lumbar intradiscal pressure. Thesis. *Acta Orthop Scand (Suppl)* 43:62-74, 1960
  19. Nachemson A, Morris J: In vivo measurements of intradiscal pressure. *J Bone Joint Surg* 46A:1077-1092, 1964
  20. Riggs BL, Melton LJ: *Osteoporosis: Etiology, Diagnosis, and Management*. New York, Raven Press, 1988, pp 119-122
  21. Roaf R: A study of the mechanism of spinal injuries. *J Bone Joint Surg* 42B:810-823, 1960
  22. Rothman RH, Simeone FA: *The Spine*. Second edition. Philadelphia, WB Saunders, 1982, pp 828-830
  23. Sandor BI: *Strength of Materials*. Engelwood Cliffs, NJ, Prentice-Hall, 1978
  24. Shirazi-Adl SA, Shirivavastava SC, Ahmed AM: Stress analysis of the disc-body unit in compression. *Spine* 9:120-134, 1984
  25. White AA, Panjabi MM: *Clinical Biomechanics of the Spine*. Philadelphia, JB Lippincott, 1978
  26. Willen J, Lindahl S, Irstam L, Aldman B, Nordwall A: The thoracolumbar crush fracture: An experimental study on instant axial dynamic loading—the resulting fracture type and its stability. *Spine* 9:624-631, 1984
  27. Yang KH, King AI: Mechanism of facet load transmission as a hypothesis for low-back pain. *Spine* 9:557-565, 1984

---

*Address reprint requests to*

Osamu Shirado, MD  
 Department of Orthopaedic Surgery  
 Hokkaido University School of Medicine  
 Kita-15 Nishi-7, Kita-Ku  
 Sapporo 060, Japan

---